Analysis of Distribution and Grouping of MRI Characteristics of Age-Related Cerebral Microangiopathy

E. I. Kremneva[a], *, M. R. Zabitova[b], K. V. Shamtieva[b], M. V. Krotenkova[a], and L. A. Dobrynina[b]

[a] Radiology Department, Research Center of Neurology, Moscow, 125367 Russia
[b] 3d Neurology Department, Research Center of Neurology, Moscow, 125367 Russia
*e-mail: kremneva@neurology.ru

Abstract—Small vessel disease (SVD) is the leading cause of vascular and cognitive impairment (CIs) mixed with neurodegeneration. MRI can shed light on SVD pathogenesis and progression mechanisms in vivo. The aim of our study is the assessment of heterogenity of MRI features (based on the STRIVE standard) in age-related SVD and its relation to disease progression mechanisms. 96 patients with age-related SVD (of different severities) (63 women; mean age, 60.6 ± 6.3 years) and 23 healthy volunteers (15 women; mean age, 58 ± 6 years) were examined. MRI scanning (3 T) for all participants included T2-WI, T1-WI, DWI, FLAIR, and SWI regimens with subsequent analysis of SVD brain lesions based on the STRIVE standards. STRIVE features were asessed using a four-point scale. The cluster analysis for Fazekas 3 patients showed two clusters of SVD MRI features. Group 1 had mostly periventricular WMHs, more lacunes, microbleeds, and brain atrophy. Group 2 did not have microbleeds and exhibited mostly juxtacortical WMH (Group 2-2) or posterior leucoaraiosis in periventricular WM with WM lacunes and enlarged perivascular spaces in the basal ganglia (Group 2-1). The combination of MRI features in each cluster probably reflects the predominance of ischemic and non-ischemic mechanisms of SVD. Our results provide evidence for different mechanisms of small brain vessels and brain parenchymal damage in SVD. Further studies are needed to see the clinical relevance.

Keywords: age-related cerebral microangiopathy, small vessel disease, MRI, STRIVE criteria, cluster analysis

DOI: 10.1134/S0362119721080119

INTRODUCTION

Cerebral microangiopathy (the synonym for "small vessel disease" (SVD)) is a set of neuroimaging—morphological and associated clinical manifestations determinated by damage to small (less than 500 μm in diameter) cerebral vessels. SVD includes numerous, both sporadic and hereditary, diseases associated with damaged small vessels. Given the technical limitations of their in-vivo imaging, SVD is diagnosed by the signs of brain lesion. The diagnostic MRI characteristics include acute or subacute small subcortical infarctions, white matter hyperintensities (WMH), lacunes, enlarged perivascular spaces (EPVS), microbleeds (MBs), brain atrophy (STandards for ReportIng Vascular changes on nEuroimaging, STRIVE, 2013) [1]. Owing to wider prevalence, the sporadic forms of age-related SVD associated with vascular risk factors make the greatest contribution to the development of vascular and neurodegeneration-related cognitive impairment (CI), stroke, disability, and death of patients [2].

It has been established that the age-related SVD and its leading MRI characteristic, WMH, are associated with arterial hypertension (AH), diabetes mellitus, smoking, hyperlipidemia, as well as cognitive decline, gait disorders, and pelvic floor dysfunction [3]. Data on the predominant role of periventricular WMH [4] or deep WMH in CI development are ambiguous [5]. It should also be CI that the WMH load is not correlated with CI severity in a considerable part of patients. Studies have shown that the increased number of lacunes (including silent lacunar lesions) and the reduced brain volume are directly related to the progression of CI, particularly those accompanied by changes in the control functions of the brain and operational performance rate [6]. Numerous studies indicate a relationship between the presence of MBs of the lobar and deep and/or mixed localization and the development of CI [7]. The large research team headed by Charidimou considers that the overall severity of MB lesions rather than their localization may be important for CI [8]. However, localization still may be useful for establishing the causes of brain lesion, because it is related to the pathological processes resulting in the appearance of MBs [9].

The ambiguous data on diagnostic and prognostic significance of the MRI indicators of SVD can be accounted for heterogeneity of the forms and mechanisms of the disease. Until recently, ischemic white matter lesions as a result of arteriolosclerosis in patients with poorly controlled AH have been consid-

Table 1. General characteristics of the group of SVD patients

Parameter	Main group ($n = 96$)
Age (M ± SD), years	61 ± 6.8
Gender (female)	64 (66.6%)
Education (M ± SD), years	14 ± 2.4
Hypertension, *n* (%)	
Stage 0	14 (14.6%)
Stage 1	9 (9.4%)
Stage 2	20 (20.8%)
Stage 3	53 (55.2%)
Diabetes mellitus, *n* (%)	19 (19.8%)
Obesity	31 (32.3%)
Smoking	24 (25%)
Cognitive impairment:	
Subjective cognitive impairment (MoCA ≥ 26)	35 (36.5%)
Mild cognitive impairment	46 (47.9%)
Dementia	15 (15.6%)

ered to be the only mechanism of brain lesion in SVD. However, the breakthroughs in AH treatment have not led to a significant decrease in the proportion of SVD and related CI in the population, which makes us to think that is not solely ischemia that plays the primary role in its development [10]. The role of endothelial lesion with increased permeability of the blood−brain barrier (BBB) as one of the mechanisms for SVD initiation and progression is being intensely discussed in literature [11].

In the present study, we have attempted to distinguish different SVD forms based on the analysis of expression and prevalence of diagnostic MRI characteristics in the cerebral lobes and differentwhite matter regions and their grouping with each other, assuming that the emergence of various forms may be a consequence of the dominance of different mechanisms of damage to white matter and can explain the incomplete correspondence between the expression of MRI characteristics and clinical manifestations of SVD.

MATERIALS AND METHODS

The one-stage complete survey design was used. The survey involved 46- to 70-year-old patients who applied to the Research Center of Neurology from January 2016, to December 2017, with cognitive copmplaints (impaired memory and concentration, mental retardation, etc.), with MRI changes corresponding to the SVD symptoms described by the STRIVE standards 2013 [1]. The patients with potential Alzheimer's disease, other causes of brain lesion, >50% atherosclerosis of the main arteries of the head and neck, severe somatic pathology, as well as contraindications for MRI, were excluded. The study involved 96 patients (63 women; the mean age, 60.6 ± 6.3 years

old). All patients underwent the general, neurological and neuropsychological examinations, assessment of activities in daily living, and MRI of the brain. The total clinical characteristics of the group are present in Table 1.

The MRI procedure. All brain scans were performed with a 3-Tesla Magnetom Verio scanner (Siemens, Erlangen, Germany) and included the following sequences: axial T2-weighted fast spin-echo (time repetition (TR), 4000 ms; time echo (TE), 118 ms; slice thickness, 5 mm); sagittal 3D FLAIR with isotropic voxel (1 × 1 × 1 mm) (TR, 6000 ms; TE, 395 ms); sagittal 3D T1-mpr (TR, 1900 ms; TE, 2.5 ms; slice thickness, 1.0 mm); axial diffusion-weighted imaging (DWI) (TR, 6600 ms; TE, 100 ms; 25 sections, slice thickness, 4 mm; 2 b-factors = 0 and 1000 s/mm²; 3 diffusion encoding directions); axial SWI (susceptibility-weighted imaging) providing 88 axial slices (TR = 28 ms; TE = 20 ms; slice thickness, 1.2 mm).

MR images were analyzed using qualitative assessment of the MRI features of SVD (Fig. 1) according to the STRIVE standards [1] by two experienced neuroradiologists (K.E.I. and A.B.M.); in case of interrater discreepancy, the data were discussed with the third neuroradiologist (K.M.V.). The analysis was performed using the eFilm Workstation 4.2.2 (IBM Watson Health, United States).

Lacunes were analyzed by T1-weighted FLAIR; their number was counted in the subcortical structures, the cerebral white matter, the brainstem and the cerebellum (with gradation for each area separately: 0/<5/5−10/>10 lacunes).

WMH was detected on T1 and FLAIR images; for the entire brain, the grade was indicated on the modified Fazekas (F) scale (F0, absence; F1, single lesions;
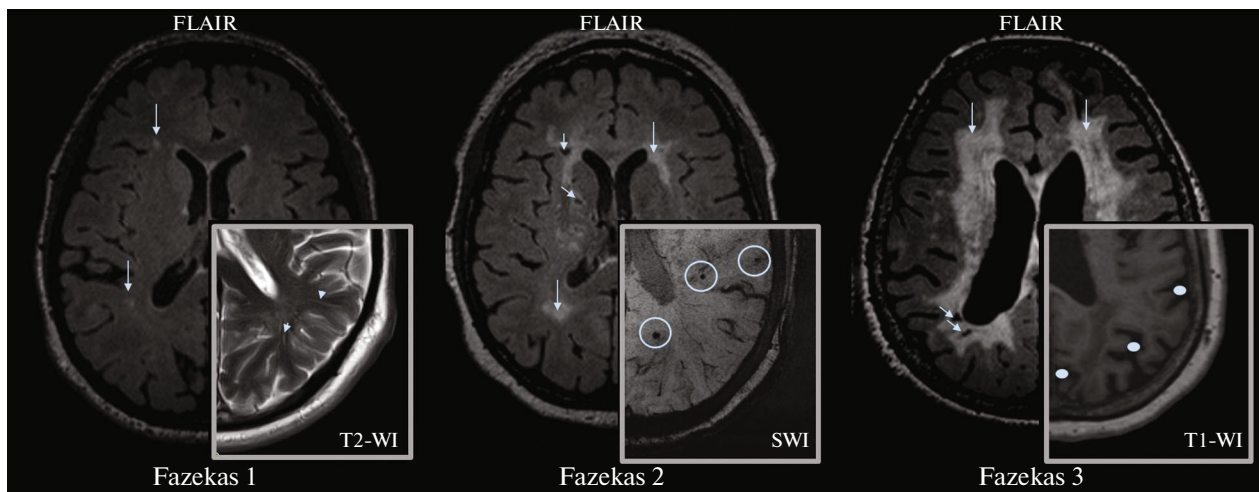
Fig. 1. The changes in white matter by the modified Fazekas scale with imaging of SVD features in the respective regimens: arrows, WMH; short arrows, lacunes; triangles, PVS; circles, MBs; points, enlargement of CSF-containing spaces as manifestation of brain atrophy.

F2, single and partially lesions; F3, confluent lesions/leukoaraiosis) [12] (Fig. 1).

In individual anatomical regions, WMH was assessed by a four-point scale (no changes/single lesions/partially confluent lesions/diffuse hyperintensity). The following regions were assessed: frontal lobes (separately for the anterior parts (the prefrontal region) and posterior parts (the premotor and motor regions)), temporal, parietal and occipital lobes, as well as hyperintensity (HI) in subcortical structures. At the same time, WMH was analyzed separately in each of the lobes in the periventricular white matter (pWM) (up to 13 mm from the walls of the lateral ventricles), in the juxtacortical WM (jWM) (up to 4 mm from the corticomedullary junction) and deep WM (dWM) (WM between pWM and jWM) [13].

Microbleeds (MBs) were estimated on SWI images. The analysis was carried out in the regions analogous to those in WMH analysis using a four-point scale in each part (number 0/<5/5−10/>10).

Brain atrophy was assessed both by the enlargement of cerebrospinal fluid (CSF) spaces grade and automatically with calculation of the cortical volume.

External CSF spaces were estimated for each lobe of the cerebral hemispheres (separately for the anterior and posterior parts of the frontal lobes) using the global cortical atrophy (GCA) scale: normal volume/slight opening of brain fissures/decreased gyral volume/icicle-type gyral atrophy [14].

The ventricles of the brain were assessed by calculating the ventricular−cranial coefficients (VCC 1−3) [15]. Additionally, the coefficient of the posterior horns of the lateral ventricles (VCC 4) was calculated: the ratio of the maximum distance between external contours of the posterior horns of the lateral ventricles to the maximum distance between the inner cranial bone plates.

The volume of the lateral ventricles and external CSF spaces was calculated using SPM12 (voxel-based morphometry (VBM) [16]) through segmentation of T1mpr images into gray matter, white matter, and cerebrospinal fluid, followed by volume calculation and normalization per total intracranial volume.

Perivascular spaces (PVS): for the centrum semiovale and subcortical structures, the number (0/<5/5−10/>10 pieces) and enlargement severity (no/1 mm/2 mm/3 mm/single of more than 4 mm) were estimated in the on T1 and FLAIR images.

The patients had no recent small infarctions according to the DWI data and, hence, this characteristic was not discussed thereafter.

Statistical analysis was performed using the IBM SPSS Statistics 23.0 software. The quantitative variables were presented as the mean $\pm$ standard (root mean square) deviation; the qualitative variables were presented as the frequency and proportion (in percent). The type of distribution of quantitative variables was assessed using frequency histograms and the Kolmogorov−Smirnov test. In all cases, the bilateral variants of statistical criteria were used. The null hypothesis was rejected at $p < 0.05$. For the dependent quantitative variables, the effect of the independent qualitative variable was assessed by the analysis of variance followed by the least significant difference test for pairwise comparisons; the χ^2 test and Fisher's exact test (if at least one expected number in the cells of the table proved to be less than 5) were used for the dependent qualitative variable. The correlations of the quantitative variables with each other were assessed by the Pearson correlation method. Hierarchical cluster analysis was used to determine the particular pattens of MR images of brain lesion in SVD patients.
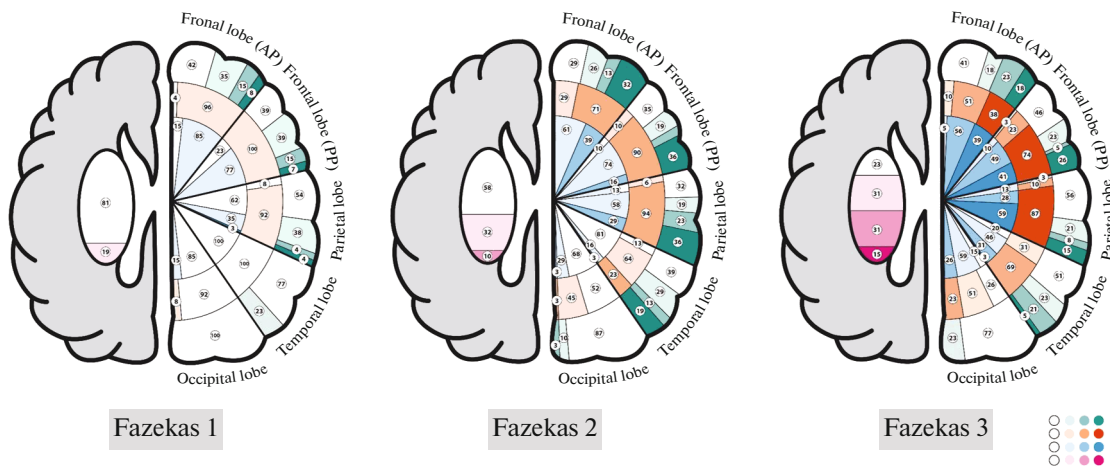
Fig. 2. The distribution of white matter hyperintensities (WMH) over anatomical regions of the brain (on the right: for the lobes of the cerebral hemispheres; on the left: for the subcortical structures) and white matter areas (on the right) for the groups of patients depending on the Fazekas stage. Green color, jWMH; orange, dWMH; blue, pWMH; pink, subcortical structures; color intensity codes for the 4-point scale of WMH load (from absence to maximum severity).

RESULTS

Total Group Analysis

WMH analysis in the entire group (96 patients, 63 women; mean age, 60.6 ± 6.3 years; 26, 31, and 39 subjects for F1, F2, and F3, respectively) showed largely the greater involvement of frontal and parietal lobes. PWMH, dWMH, and jWMH of more than 2 points in the frontal lobes was 51%, 59.4%, 37.5% (anterior regions) and 41.7%, 68.7%, 33.3% (posterior regions), respectively; in the parietal lobes, they were 45.8%, 69.8%, and 27.1%, respectively.

MBs were detected in 37 subjects (38.5%): the jWM/cortex, 5 subjects (5.2%); the basal ganglia, 8 subjects (8.33%); pWM and dWB, 3 subjects (3.21%); mixed-location (jWM + basal ganglia), 21 subjects (21.88%).

The enlargement of **external CSF spaces** was shown in the frontal lobes (the anterior and posterior parts): slight in 53.1% and 47.9% and moderate in 6.3% and 3.1%, respectively; in the parietal lobes: slight in 34.4%; in the temporal and occipital lobes: slight in 15.6% and 7.3%, respectively.

PVS (>10) were imaged in the centra semiovale of 97.9% patients and in the subcortical structures of 100% patients. PVS > 2 mm in the subcortical structures and the centra semiovale were detected in 28 (29.2%) and 4 (4.2%) patients; in other patients, they were 1−2 mm in size.

Lacunes were detected in 49.3% patients, in half of cases, in two or more regions. They were localized in the white matter of cerebral hemispheres in 43.7% patients, in the subcortical structures in 33.3% patients, in the brainstem in 28.1% patients, and in the cerebellum in 18.7% patients.

Fazekas Subgroup Analysis

In enrolled participants , the WMH of stages F1, F2, and F3 was detected in 26 (27.1%), 31 (32.3%), and 39 (40.6%) subjects, respectively. The patients had no age differences. Women were prevalent in the subgroups with F1 and F2; for F3, gender-related distribution was approximately the same.
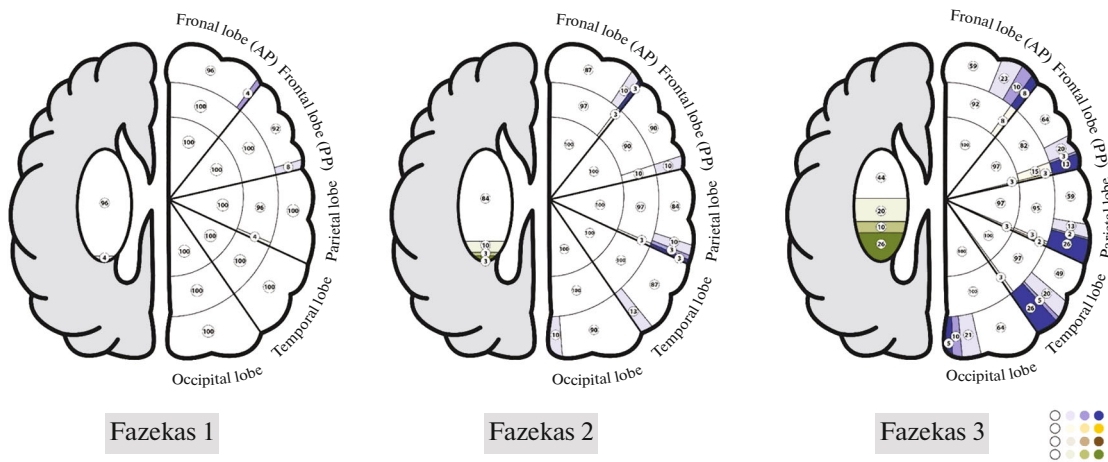
In the brain lobes and white matter regions , WMH increased with the F stage in pWM and dWM of the frontal lobes and over the entire white matter of other parts of cerebral hemispheres. In frontal jWM, there was no statistically significant difference between F groups. The maximum WMH load was observed in the frontal and parietal lobes (Fig. 2). The significant increase in HI was found in subcortical structures with the more severe F stage.

The number of **MBs** significantly decreased with the F stage in jWM of all lobes and in subcortical structures (Fig. 3). MBs were already present at the F1 stage in jWB of the anterior and posterior parts of the frontal lobes in 4% and 8%, respectively, and subcortical structures, in 4%. At the F2 and F3 stages, the evidence of MBs in these areas increased and they were detected in jWB of the posterior parts of the cerebral hemispheres (Fig. 3).

Significant differences in **external CSF space** volumes between F groups were observed only in the parietal lobes.

The multiple comparisons of all **VCCs** showed significant differences between F3 and F1, F3 and F2.

The volumes of brain and CSF relative to the entire intracranial volume, gray and white matter relative to the entire brain volume showed significant differences between the groups of F stages (Fig. 4). A significant decrease in gray and white matter volumes compared to other groups was shown only for stage F3.

Fig. 3. The distribution of microbleeds (MBs) over anatomical regions of the brain (on the right: for the lobes of the cerebral hemispheres; on the left: for the subcortical structures) and white matter areas (on the right) for the groups of patients according to Fazekas. Blue, juxtacortical MBs; yellow, deep MBs; brown, periventricular MBs; green, subcortical structures; color intensity codes for the 4-point scale of MB load (from absence to maximum severity).
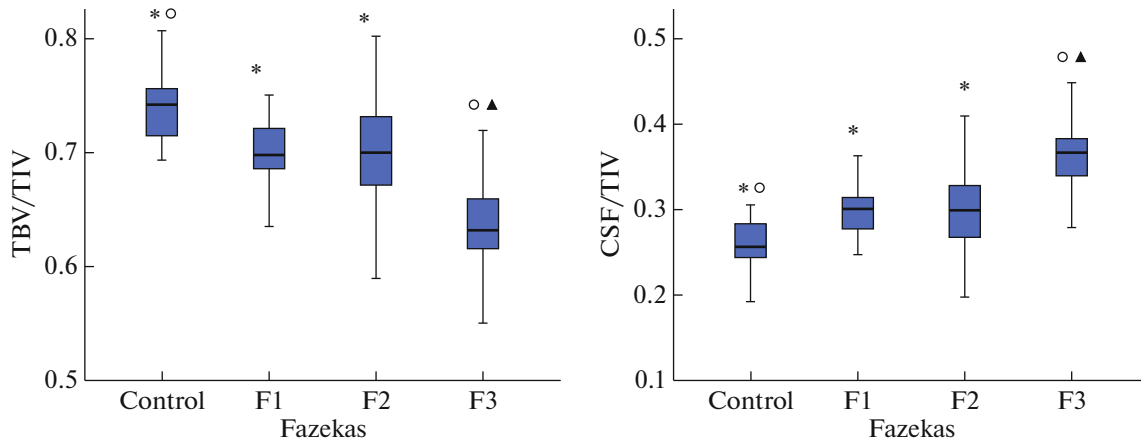
Fig. 4. The difference between total brain and cerebrospinal fluid volumes normalized per intracranial volume (TBV/TIV (total brain volume/total intracranial volume) and CSF/TIV (cerebrospinal fluid volume/total intracranial volume)) in the Fazekas groups and in the control. Statistically significant differences ($p \leq 0.05$) with the groups are marked with an asterisk for F3, a circle for F2, and a triangle for F1.

With respect to the **PVS** number in the centra semiovale and subcortical structures, F groups had no differences, while the sizes of perivascular spaces in subcortical structures were reliably higher in the patients with F3 compared to F1 and F2.

The statistically significant difference between F groups in the number of **lacunes** was shown both for the white matter and for the subcortical structures, the brainstem and the cerebellum (Fig. 5).

Cluster Analysis

The cluster analysis for separate estimated parameters of MR images revealed the two groups of patients (Fig. 6); two patients could be assigned to neither of the clusters due to limitations of their scanning proto-

cols. The first cluster included 18 subjects (mean age, 59.1 ± 6.8 years, 6 women); the second one contained 76 subjects (mean age, 61.0 ± 6.8 years, 56 women). At the same time, all the 18 subjects from the first cluster belonged to F3, while the second cluster included the patients both with F3 (22 subjects) and with F2 (28) and F1 (26). Taking into account disproportionate division of the above clusters with respect to lesion size and severity, the subsequent analysis of the clusters was performed among the patients with F3 (group 1 (G1) and group 2 (G2)). In G2, the mean age was 63.5 ± 6.2 years, 15 women. The groups were not significantly different in AH severity and age.

G1, compared to G2, showed a significant ($p \leq 0.05$) predominance of the pWMH volume in the frontal, temporal and occipital lobes and dWMH vol-
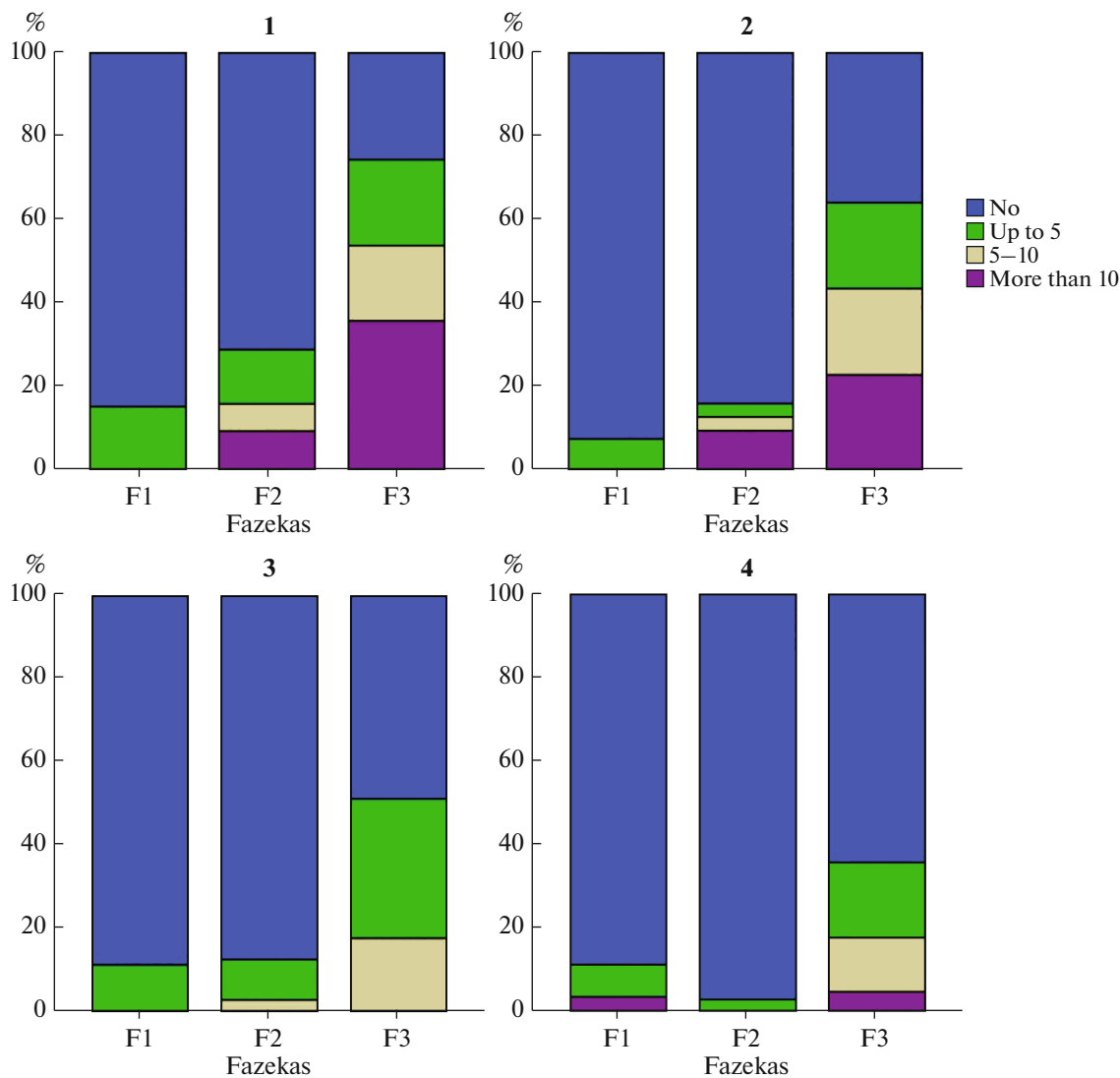
Fig. 5. The distribution of the number of lacunes in different parts of the brain depending on the Fazekas stage: **1**, in the white matter; **2**, in the subcortical structures; **3**, in the brainstem; **4**, in the cerebellum; blue, no lacunes; green, up to 5 lacunes; yellow, 5–10 lacunes; purple, more than 10 lacunes.

ume in the occipital lobes; HI in the subcortical structures and in the brainstem; the number of MBs in jWM of all lobes, as well as in the subcortical structures; slight enlargement of external CSF spaces of the parietal, temporal and occipital lobes; the number of lacunes in white matter of the cerebral hemispheres, the subcortical structures, the brainstem; the VCC2, VCC3, VCC4 values.

Then each of the above groups (G1 and G2) underwent a separate cluster analysis with dividing into subclusters. G1-1 (8 subjects) and G1-2 (9 subjects) were identified within G1, and their comparison showed the statistically significant predominance of the number of MBs in jWM of the anterior and posterior parts of the frontal lobes, the parietal, temporal

and occipital lobes in G1-2. In G2, subgroups G2-1 (14 subjects with the mean age of 62.5 ± 7.4 years, 5 men and 9 women) and G2-2 (8 subjects with the mean age of 65.1 ± 3 years, 2 men and 6 women) were identified. The comparison of these subgroups showed the statistically significant predominance of the number of HI in jWM of the anterior and posterior parts of the frontal lobes, the parietal, temporal and occipital lobes in the G2-2 group; the G2-1 group was characterized by the predominance of lacunes in white matter of the cerebral hemispheres and the tendency to predominance of HI in pWM of the temporal lobes ($p = 0.052$) and enlarged PVSs in subcortical structures ($p = 0.058$).
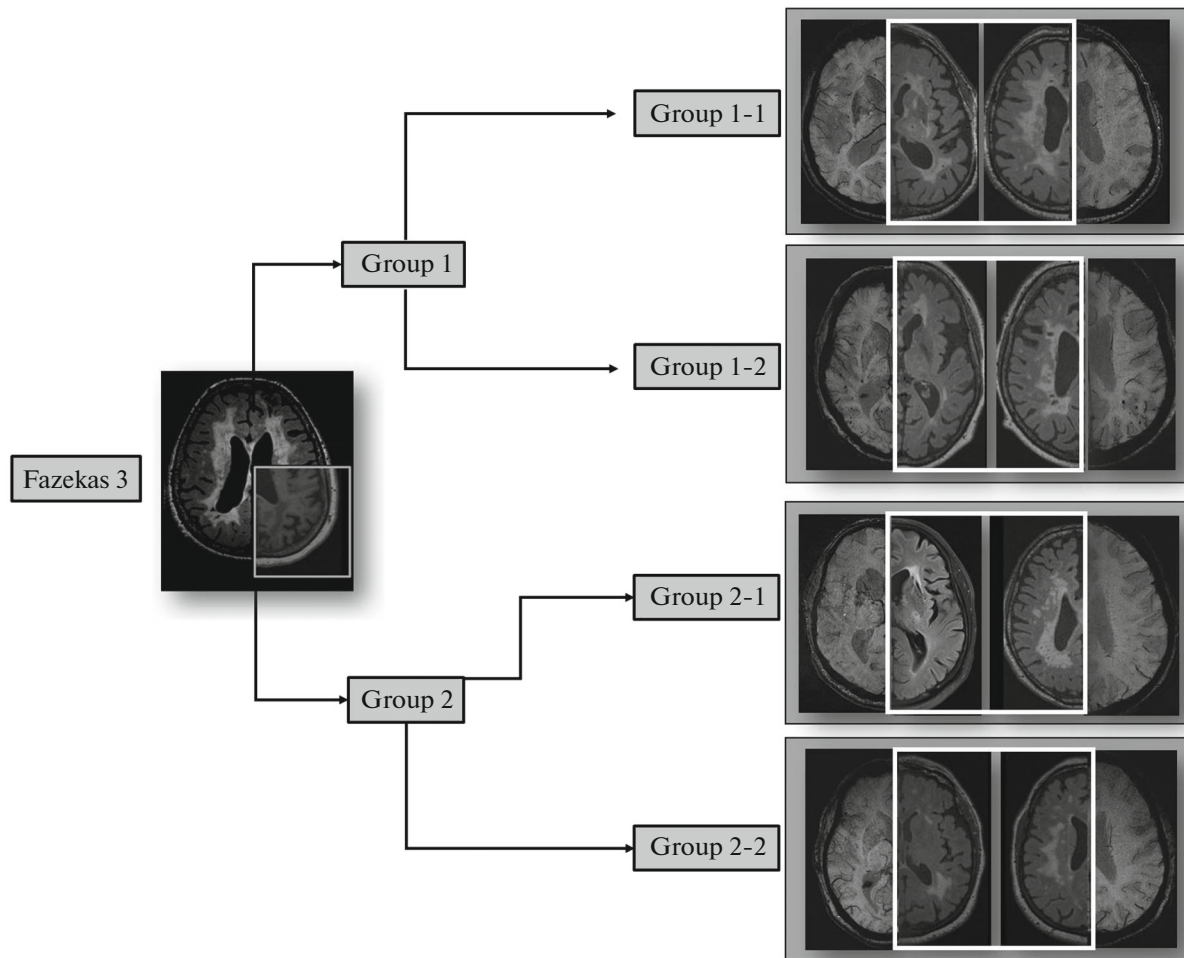
Fig. 6. The typical MRI changes (according to the data of SWI and FLAIR sequences (in the white square)) in the subgroups of patients with Fazekas 3 identified by the cluster analysis.

DISCUSSION

The pathogenetic concept of sporadic SVD generally accepted since the middle of the 20th century, when this disease was associated solely with AH and brain parenchyma ischemia as the only mechanism of brain damage, is currently being reconsidered and updated [17]. The latest data of different studies demonstrate an important role of other mechanisms, such as early endothelial dysfunction with high BBB permeability [18]. Most probably, the predominance of particular mechanisms of small vessels and brain damage causes incomplete discrepancy in the severity of clinical and MRI manifestations. Considering the crucial importance of MRI features of SVD in its diagnostics, we have analyzed the severity and distribution of MRI features in the lobes of the cerebral hemispheres and white matter areas to detect the MRI forms of SVD.

It has been shown that WMH manifests itself largely in the frontal and parietal lobes, nonuniformly over the entire white matter, damaging primarily its deep parts (Fig.2). It is believed that these parts of WM, being an intracerebral zone of watershed blood supply, are most susceptible to hypoxia and ischemia as a result of arteriolosclerosis and the loss of myocytes of the tunica media of cortical-medullary arteries [19]. The extreme manifestation of ischemia in these zones is the formation of lacunes (lacunar infarcts). Their number increases along with the progressing damage to white matter and is confirmed by the correlation between the reduced arterial blood flow, according to phase-contrast MRI, and the increased number of lacunes, like in this sample of patients [20]. On the other side, there are numerous literature data showing that WMH in SVD can be partly related to another mechanism: the higher BBB permeability and the impaired drainage of interstitial fluid with swelling of the brain parenchyma [21]. This mechanism of SVD development is indicated by the presence in our sample of patients with mutiple enlarged PVSs in the basal

ganglia surrounded by HI, and mainly jWBH. The juxtacortical WM is supplied with blood better compared to the deep WM; therefore, jWMH formation cannot be explained by ischemia. An interesting finding was that some patients at the F1 stage were shown to have MBs which, according to the ischemic concept, are the marker of evident changes in vessels and must be accompanied by considerable changes in WM, as is shown by MRI data, which suggests another mechanism of their formation.

The important finding of our study is as follows: in more than half of all 37 patients with MBs and AH of different severity, MBs were localized both in the deep and superficial areas of the brain; at the same time, according to the classical concepts, in case of hypertensive encephalopathy MBs are localized in subcortical structures. All patients with the maximum number of MBs belonged to cluster 1 with the maximum severity of WMH in pWM of the anterior and posterior parts of the frontal lobes, the temporal and occipital lobes; in dWM of the occipital lobes; and the maximum number of lacunes in white matter of the cerebral hemispheres, the subcortical structures and the brainstem. This means that our sample of MB patients did neither satisfy the generally accepted criteria of CAA, according to which the presence of lacunes is untypical and WMH is localized mainly in the posterior parts of the brain hemispheres [22]. Such situation can indicate that the juxtacortical/cortical localization of MBs is most likely not the prerogative of only amyloid-induced damage to cortical vessels. At present, more and more studies show that SVD is quite often characterized by mixed localization of MBs, where one of the mechanisms may be venous congestion, swelling and microruptures of cortical venules [20, 23], rather than the lesion of cortical arteries, as in the case of CAA.

We have demonstrated significant differences between F3 and F1, F2 groups in the size of PVSs localized in subcortical structures. It is believed that the increase of arterial pulsation, with obstruction of the drainage of interstitial fluid in PVSs, manifests with PVS enlargement and formation of WMH. In this case, WMH represents congestion phenomena due to remodeling and reduction in elasticity of the veins as a result of propagation of the pulse wave poorly damped by stiff arterial walls [24, 25]. Such changes, i.e., the enlargement of PVSs of subcortical structures against the background of WMH, have been observed in some of our patients from group 2.

The cluster analysis performed in the present work has revealed the two major MRI types of Fazekas 3 SVD. In group 1, there was a significant predominance of extended pWMH, HI in the subcortical structurtes and in the brainstem, a great number of lacunes, the presence of MBs, which was accompanied by brain atrophy; at the same time, some of the patients in this group reliably differed in the number of juxtacortical MBs (subgroup 1−2). In group 2, MBs were absent, some patients had mainly jWMHs (subgroup 2−2) and others were characterized mainly by the posterior WMH: in pWM of the temporal and parietal lobes, in combination with lacunes in WM of the cerebral hemispheres and enlarged PVSs in the basal ganglia (subgroup 2−1). At the same time, there were no significant differences between the groups in the severity of either AH or CI. The array of the MRI features in group 1 indicates the more severe brain parenchima damage (as manifestation of the more generalized damage to vessel walls) comapred to group 2. At the same time, the revealed characteristics of MRI features of group 2, in particular, enlarged PVSs in subcortical structures and predominance of jWMH (in the areas with sufficient blood supply), corresponds more to the mechanism of BBB damage and increased permeability, which has been actively discussed in literature in recent years [26].

CONCLUSIONS

The analysis of the intensity and distribution of diagnostic MRI features over the cerebral hemispheres and white matter areas, as well as their grouping in the cluster analysis, reveals heterogeneity of SVD forms. The combination of MRI features established for different forms is indicative of differences in the predominant mechanisms of disease development, and it requires thorough comparisons with the clinical manifestations and multimodal studies with assessment of tentative mechanisms. Specification of the pathogenetic variants of SVD in future will contribute to the development of individual strategy of effective treatment to prevent the progression of this disease, including preclinical stage.

COMPLIANCE WITH ETHICAL STANDARDS

All procedures performed in studies involving human participants were in accordance with the ethical standards of the institutional and/or national research committee and with the 1964 Helsinki Declaration and its later amendments or comparable ethical standards.

INFORMED CONSENT

Informed consent was obtained from all individual participants involved in the study.

CONFLICT OF INTEREST

The authors declare that they have no conflicts of interest.

REFERENCES

1. Wardlaw, J.M., Smith, E.E., Biessels, G.J., et al., Neuroimaging standards for research into small vessel disease and its contribution to ageing and neurodegeneration, *Lancet Neurol.*, 2013, vol. 12, pp. 822−838.
https://doi.org/10.1016/S1474-4422(13)70124-823867200

2. Gorelick, P.B., Scuteri, A., Black, S.E., et al., Vascular contributions to cognitive impairment and dementia: a statement for healthcare professionals from the American Heart Association/American Stroke Association, *Stroke*, 2011, vol. 42, pp. 2672−2713. PMID:
https://doi.org/10.1161/STR.0b013e318229949621778438

3. Wright, C.B., Festa, J.R., Paik, M.C., Schmiedigen, A., Brown, T.R., Yoshita, M., et al., White matter hyperintensities and subclinical infarction: associations with psychomotor speed and cognitive flexibility, *Stroke*, 2008, vol. 39, pp. 800−805.
https://doi.org/10.1161/STROKEAHA.107.
48414718258844

4. Kloppenborg, R.P., et al., Presence and progression of white matter hyperintensities and cognition: a meta-analysis, *Neurology*, 2014, vol. 82, no. 23, pp. 2127−2138.
https://doi.org/10.1212/WNL.00000000000005052481
4849

5. Smith, C.D., Johnson, E.S., van Eldik, L.J., Jicha, G.A., Schmitt, F.A., Nelson, P.T., Kryscio, R.J., Murphy, R.R., and Wellnitz, C.V., Peripheral (deep) but not periventricular MRI white matter hyperintensities are increased in clinical vascular dementia compared to Alzheimer's disease, *Brain Behav.*, 2016, vol. 6, no. 3, p. e00438.
https://doi.org/10.1002/brb3.43826925303

6. Benjamin, P., et al., Strategic lacunes and their relationship to cognitive impairment in cerebral small vessel disease, *NeuroImage: Clin.*, 2014, vol. 4, pp. 828−837.
https://doi.org/10.1016/j.nicl.2014.05.00924936433

7. Yakushiji, Y., et al., Basal ganglia cerebral microbleeds and global cognitive function: the Kashima Scan Study, *J. Stroke Cerebrovasc. Dis.*, 2015, vol. 24, no. 2, pp. 431−439.
https://doi.org/10.1016/j.jstrokecerebrovas-dis.2014.09.01525516488

8. Charidimou, A., Gang, Q., and Werring, D.J., Sporadic cerebral amyloid angiopathy revisited: recent insights into pathophysiology and clinical spectrum, *Neurol. Neurosurg. Psychiatry*, 2012, vol. 83, no. 2, pp. 124−137.
https://doi.org/10.1136/jnnp-2011-30130822056963

9. Charidimou, A., et al., White matter perivascular spaces on magnetic resonance imaging: marker of cerebrovascular amyloid burden? *Stroke*, 2015, vol. 46, no. 6, pp. 1707−1709.
https://doi.org/10.1161/STROKEAHA.115.
00909025908461

10. Shi, Y., et al., Cerebral blood flow in small vessel disease: a systematic review and meta-analysis, *J. Cereb. Blood Flow Metab.*, 2016, vol. 36, no. 10, pp. 1653−1667.
https://doi.org/10.1177/0271678X1666289127496552

11. Wardlaw, J.M., et al., Blood-brain barrier failure as a core mechanism in cerebral small vessel disease and dementia: evidence from a cohort study, *Alzheimer's Dementia*, 2017, vol. 13, no. 6, pp. 634−643. PMCID: PMC5472180
https://doi.org/10.1016/j.jalz.2016.09.006

12. Pantoni, L., Basile, A.M., Pracucci, G., Asplund, K., Bogousslavsky, J., Chabriat, H., et al., Impact of age-related cerebral white matter changes on the transition to disability: the LADIS study: rationale, design and methodology, *Neuroepidemiology*, 2005, vol. 24, pp. 51−62.
https://doi.org/10.1159/00008105015459510

13. Kim, K.W., MacFall, J.R., and Payne, M.E., Classification of white matter lesions on magnetic resonance imaging in the elderly, *Biol. Psychiatry*, 2008, vol. 64, no. 4, pp. 273−280.
https://doi.org/10.1016/j.biopsych.2008.03.024

14. Pasquier, F., Leys, D., Weerts, J.G., et al., Inter- and intraobserver reproducibility of cerebral atrophy assessment on MRI scans with hemispheric infarcts, *Eur. Neurol.*, 1997, vol. 36, no. 5, pp. 268−272.
https://doi.org/10.1159/0001172708864706

15. Gubskii, L.V., Erokhina, L.G., Vavilov, S.B., et al., *Rentgenovskaya komp'yuternaya tomografiya v nevrologii. Metodicheskoe posobie dlya studentov meditsinskikh institutov* (X-Ray Computed Tomography in Neurology: Practical Manual for Students of Medical Institutions), Moscow: Ross. Gos. Med. Univ., 1994.

16. Ashburner, J. and Friston, K.J., Voxel-based morphometry—the methods, *NeuroImage*, 2000, vol. 11, no. 6, pp. 805−821.
https://doi.org/10.1006/nimg.2000.0582

17. Fisher, C.M., The arterial lesions underlying lacunes, *Acta Neuropathol.*, 1969, vol. 12, pp. 1−15.

18. Shim, Y.S., Yang, D.W., Roe, C.M., et al., Pathological correlates of white matter hyperintensities on magnetic resonance imaging, *Dementia Geriatr. Cognit. Disord.*, 2015, vol. 39, nos. 1−2, pp. 92−104.
https://doi.org/10.1159/00036641125401390

19. De Reuck, J., The human periventricular arterial blood supply and the anatomy of cerebral infarctions, *Eur. Neurol.*, 1971, vol. 5, no. 6, pp. 321−334.

20. Akhmetzyanov, B.M., The role of blood flow and CSF flow disorders in brain damage during cerebral microangiopathy, *Cand. Sci. (Med.) Dissertation*, Moscow, 2019.

21. Dobrynina, L.A., Age-related neurovascular interaction and cerebral perfusion during cerebral microangiopathy and Alzheimer's disease, *Ann. Klin. Eksp. Nevrol.*, 2018, vol. 12, no. 5, pp. 87−94.
https://doi.org/10.25692/ACEN.2018.5.11

22. Greenberg, S.M. and Charidimou, A., Diagnosis of cerebral amyloid angiopathy evolution of the Boston criteria, *Stroke*, 2018, vol. 49, pp. 491−497.
https://doi.org/10.1161/STROKEAHA.117.016990

23. Dobrynina, L.A., Akhmetzyanov, B.M., Gadzhieva, Z.Sh., Kremneva, E.I., Kalashnikova, L.A., and Krotenkova, M.V., The role of impaired arterial, ve-

nous and CSF flow in the development of cognitive disorders during cerebral microangiopathy, *Ann. Klin. Eksp. Nevrol.*, 2019, vol. 13, no. 2, pp. 19−31.
https://doi.org/10.25692/ACEN.2019.2.3

24. Potter, G.M., Doubal, N., Jackson, C.A., et al., Enlarged perivascular spaces and cerebral small vessel disease, *Int. J. Stroke*, 2015, vol. 10, pp. 376−381. PMID: .
https://doi.org/10.1111/ijs.1205423692610

25. van Sloten, T.T., Protogerou, A.D., Henry, R.M., et al., Association between arterial stiffness, cerebral small vessel disease and cognitive impairment: a systematic review and meta-analysis, *Neurosci. Biobehav.*, 2015, vol. 53, pp. 121−130.
https://doi.org/10.1016/j.neubiorev.2015.03.01125827412

26. Zabitova, M.R., Shabalina, A.A., Dobrynina, L.A., Kostyreva, M.V., Akhmetzyanov, B.M., Gadzhieva, Z.Sh., et al., Tissue plasminogen activator and MRI manifestations of cerebral microangiopathy, *Ann. Klin. Eksp. Nevrol.*, 2018, vol. 12, no. 4, pp. 30−36.

Translated by E.V. Makeeva